Lesquerella seed yield estimation using color image segmentation to track flowering dynamics in response to variable water and nitrogen management

K.R. Thorp [a,*], G. Wang [b], M. Badaruddin [c], K.F. Bronson [a]

[a] USDA-ARS, U.S. Arid Land Agricultural Research Center, 21881 N Cardon Ln, Maricopa, AZ 85138, United States
[b] Bridgestone Americas Agricultural Operations, 4140 West Harmon Road, Eloy, AZ 85131, United States
[c] Maricopa Agricultural Center, University of Arizona, 37860 West Smith-Enke Road, Maricopa, AZ 85138, United States

ARTICLE INFO

ABSTRACT

Seed oil from lesquerella (*Physaria fendleri* (Gray) O'Kane & Al-Shehbaz) can potentially supplement castor oil as a non-petroleum-based chemical feedstock in the production of many industrial products. However, before lesquerella will become commercially viable, further efforts are needed to address crop management challenges and to improve lesquerella varieties. Because lesquerella develops vibrant yellow flowers on top of the canopy, digital imaging can be used to track the dynamics of its indeterminate flowering period. The objective of this study was to investigate a digital image analysis approach to (1) assess differences in lesquerella flowering dynamics due to variable water and nitrogen (N) management and (2) estimate lesquerella seed yield from flowering data. During the winters of 2011–2012 and 2012–2013, field experiments tested lesquerella responses to two irrigation levels and six N fertilization rates at Maricopa, Arizona. Biomass was sampled within a 30 cm × 30 cm area twice per month, and lesquerella flowers were manually counted. Twice per week, digital images were collected with a commercial digital camera at a nadir view angle approximately 2 m above the canopy. To obtain the percentage of yellow flowers in each image, an analysis routine included (1) an image transformation to the hue, saturation, and intensity (HSI) color space and (2) a Monte Carlo approach to address uncertainty in HSI parameters used for image segmentation. The imposed irrigation and N fertilization treatments led to differences in both flower count and flower cover ($p < 0.05$). However, the digital imaging approach permitted more frequent measurements, which revealed fine temporal changes in flowering patterns that could be explained by management factors. Due in part to the larger sampling area for the digital imaging approach, lesquerella seed yield was better estimated using flower cover percentage ($r^2 \leq 0.84$) from images as compared to manual flower counts ($r^2 \leq 0.56$). Overall, the digital imaging approach provided useful information on lesquerella flowering dynamics, which was affected by water and N management and highly correlated with seed yield.

Published by Elsevier B.V.

1. Introduction

Lesquerella (*Physaria fendleri* (Gray) O'Kane & Al-Shehbaz, formerly *Lesquerella fendleri* (Gray) Wats.) grows natively in a wide range of soil types, temperature regimes, and elevations throughout the southwestern United States and northern Mexico. Due to the abundance of hydroxylated fatty acids in lesquerella seed oil, the domestication of lesquerella as an agricultural crop began in 1960 (Smith et al., 1961). The primary fatty acid from lesquerella

seed is lesquerolic acid (14-hydroxyeicosa-11-enoic acid; C20:1-OH) (Dierig et al., 2006). This compound is similar to ricinoleic acid (12-hydroxyoctadeca-9-enoic acid; C18:1-OH), which is derived from the seeds of castor oil plants (*Ricinus communis* L.). The two compounds thus share similar uses as non-petroleum-based chemical feedstocks in the production of many industrial products: greases, lubricants, paints, inks, hydraulic fluids, and motor oils (Dierig et al., 1993). Additionally, the oils find use as a fuel additive to improve the lubricity of ultra-low-sulfur diesel, now mandated in many countries to improve air quality by reducing emissions from diesel engines (Geller and Goodrum, 2004; Moser et al., 2008). Lesquerella seed oil offers several advantages over caster oil: (1) opportunities to reduce caster oil imports through

* Corresponding author.
  E-mail address: kelly.thorp@ars.usda.gov (K.R. Thorp).

domestic lesquerella production in the southwestern United States and (2) reduced exposure to the toxic substance, ricin, found in castor seeds and seed meal. Although lesquerella is well-adapted to the arid environmental conditions of the southwestern United States, further lesquerella breeding efforts and improvements in agronomic practices are required before the crop will become commercially viable (Dierig et al., 2011).

Since the early 1990's, multiple field investigations have addressed agronomic issues associated with lesquerella production. Irrigation requirements were studied by Hunsaker et al. (1998) in Arizona and Puppala et al. (2005) in New Mexico. Both studies showed that maintaining soil water depletion above 50% was critical for maximum crop growth and seed yield. A fertilization study in Arizona showed that nitrogen (N) rates as high as 180 kg N ha^{-1} increased lesquerella seed yield, although oil content decreased as N fertilizer increased (Nelson et al., 1999). A more recent study showed optimum lesquerella seed yield with N rates between 210 and 280 kg N ha^{-1} (Liu et al., 2014). In the latter study, use of a sudangrass (*Sorghum bicolor* (L.) Moench var. sudanense) cover crop in the summer prior to lesquerella field experiments may have contributed to the higher N requirement. Other field studies have assessed herbicide tolerance (Roseberg, 1993, 1996), planting date effects (Dierig et al., 2012; Nelson et al., 1996), and climate effects at four elevations in Arizona (Dierig et al., 2006) and at a location in Argentina (Ploschuk et al., 2003).

As a technological aid for lesquerella management and breeding efforts, lesquerella canopy imaging approaches have been developed to monitor its indeterminate flowering process (Adamsen et al., 2000, 2003; Thorp and Dierig, 2011). The endeavor is facilitated by the crop's brilliant yellow flowers, which are prominently displayed on top of the lesquerella canopy. Adamsen et al. (2000) used a commercial digital camera to collect images from a nadir view angle at 1.6 m above a lesquerella canopy and developed an automatic image segmentation algorithm to identify lesquerella flowers based on assessments of the red (R), green (G), and blue (B) pixel values. Image segmentation is the process of defining regions that share similar spectral characteristics within the image. The percentage of image pixels segmented as flowers (i.e., flower cover percentage) was able to estimate flower counts with a root mean squared error (RMSE) of 235 flowers. The approach was later used by Adamsen et al. (2003) to monitor effects of N fertilizer and planting density on lesquerella flowering and to relate flowering patterns with seed yield. More recently, Thorp and Dierig (2011) developed a new image segmentation algorithm that converted RGB data to the hue (H), saturation (S), and intensity (I) color space prior to image segmentation. This transformation decoupled the intensity (or brightness) information from the color information in the images, which permitted segmentation on the more relevant color parameters of hue and saturation. The approach also incorporated a Monte Carlo scheme for assessing uncertainty in HSI parameters and its effect on flower cover calculations. Flower cover with the new approach estimated lesquerella flower counts with RMSE of 159 flowers, a 32% improvement compared to the Adamsen et al. (2000) method. However, further efforts are needed to demonstrate practical uses of the imaging technology, including crop yield prediction and assistance with management or breeding decisions.

Lesquerella field studies were recently conducted in central Arizona to evaluate responses of lesquerella seed yield and oil content to irrigation and N fertilizer management (Liu et al., 2014). As a result of imposed variability in water and N management, lesquerella flowering dynamics were highly variable both spatially and temporally. Thus, the experimental field was appropriate to conduct further testing of flower segmentation algorithms and to demonstrate practical applications of the imaging technology. The objectives were to use the Thorp and Dierig (2011) imaging approach to (1) assess lesquerella flowering responses to variable irrigation and N fertilizer management and (2) estimate lesquerella seed yield from in-season flowering patterns.

2. Materials and methods

2.1. Field experiments

Lesquerella was grown at the University of Arizona's Maricopa Agricultural Center (MAC) near Maricopa, Arizona (33.068° N, 111.971° W, 360 m above mean sea level) over the winters of 2011–2012 and 2012–2013. The soil texture at the site was Casa Grande sandy loam and sandy clay loam, classified as fine-loamy, mixed, hyperthermic, Typic Natrargids. Lesquerella (cv. "Gail") was broadcast-planted into laser-leveled seed beds on 3 November 2011 and 13 November 2012. A split plot design with four replications was established to test lesquerella growth responses to two irrigation levels (main plots) and six N fertilizer levels (subplots). Due to the limitations of flood irrigation, the irrigation treatments were not randomized. The well-watered (WW) treatment received 1288 and 1377 mm of irrigation in 2011–2012 and 2012–2013, respectively. The water-limited (WL) treatment received approximately 30% less water with deficits imposed from February to May in both years. Six N fertilizer levels (0, 56, 112, 168, 224, and 336 kg N ha^{-1}) were randomized within main plots to test effects on lesquerella growth and seed yield. Granular prilled urea (460 g N kg^{-1}) was manually applied to each 7 m × 13 m plot in five split applications: pre-planting, 6–10 leaf stage, first flower, one month after first flower, and two months after first flower. Further experimental details are provided by Liu et al. (2014).

2.2. Field measurements

Within each treatment plot, areas were designated for (1) destructive plant sampling and (2) preservation for seed yield measurements. In the destructive plant sampling areas, biomass samples were collected twice per month using a 30 cm × 30 cm frame fabricated from PVC tubing to delineate the sample area. As described by Liu et al. (2014), a variety of measurements were determined from the biomass samples, but this study required only the number of flowers within the sample (i.e., flower counts). Flower count measurements were available for seven sampling dates from 9 March to 8 June in 2012 and for five sampling dates from 25 March to 22 May in 2013. In the final harvest areas, seed yield measurements were obtained by manually harvesting and threshing biomass samples from three 1.0 m × 0.5 m areas on 20 June 2012 and 11 June 2013.

A digital camera (PowerShot G12, Canon USA, Inc., Melville, NY, USA) was used to collect images over the lesquerella canopy. The camera was equipped with a 10.0 megapixel, 7.6 mm × 5.7 mm charge coupled device (CCD) for detection and a color filter array for separation of three primary colors (RGB). Three-band images with 16-bit color depth on each channel and resolution of 3648 × 2736 pixels were collected and saved to an onboard flash memory card in the RAW image format.

An L-shaped, adjustable metal pole constructed from 2.54 cm square tubing was used to suspend the camera at a nadir view angle over the lesquerella canopy. On each image collection outing, the metal pole was adjusted to maintain a camera height of 196 cm above the ground. A wireless remote control device (WR-100 D12352B, Satechi, San Diego, CA, USA) was used to trigger the shutter on the mounted camera.

Immediately prior to biomass sampling on each sampling date, digital images were collected over the sampling area in each plot.

The 30 cm × 30 cm PVC frame was placed within the canopy prior to image collection, so the area selected for sampling was delineated in the digital images. Prior research highlighted the need to synchronize digital image collection with biomass sampling and flower counts, because lesquerella flowering is a very dynamic process (Thorp and Dierig, 2011). Thus, biomass samples were collected within 10 min after image collection. With a total of 48 plots in the experimental design for both years, 48 images and 48 biomass samples were collected on each sampling date.

Additional digital images were collected over the final harvest areas in each plot. While images over biomass sampling areas were used to calculate correlations between flower cover and flower counts, images over the final harvest areas were used to track flowering patterns in each plot over the entire growing season. Three images were collected over the final harvest areas on each outing, which generally occurred twice per week. Final harvest areas were imaged on 21 occasions from 9 March to 8 June 2012 and on 17 occasions from 19 March to 23 May 2013. The frequency of these image collection outings was necessary to monitor the crop's dynamic flowering process.

2.3. Image processing

The image processing algorithm developed by Thorp and Dierig (2011) was used to process digital images of the lesquerella canopy in this study. The algorithm converted the RGB image data to the HSI color space. Image segmentation occurred by thresholding the images using six parameters: the minimum and maximum values for H, S, and I that corresponded to flower pixels in the images. This step produced a binary image with flower pixels separated from soil background and green vegetation. A 5 × 5 median filter convolution was used on the binary image for noise reduction and smoothing. Flower cover was calculated as the percentage of image pixels identified as flowers. Further details on this image processing methodology can be found in Thorp and Dierig (2011) and Gonzalez and Woods (1992).

Image processing algorithms were developed in the Interactive Data Language (IDL) within the Environment for Visualizing Images (ENVI 4.8, Exelis Visual Information Solutions, Boulder, CO, USA). An interactive color image segmentation tool with graphical user interface was also designed to facilitate user activities, including (1) supervised image segmentation to determine HSI parameter values, (2) testing effects of HSI parameters on segmentation quality, and (3) assessments of HSI parameter uncertainty effects using a Monte Carlo sampling approach.

To process the images collected over biomass sampling areas, native ENVI algorithms were used to manually draw regions of interest (ROIs) to mark the image pixels delineated by the 30 cm × 30 cm PVC frame. Further processing of these images focused only on the area within the ROI. Supervised image segmentation was then conducted on each image by interactively selecting pixels that represented lesquerella flowers. After selecting a new flower pixel, the segmentation tool would readjust the minimum and maximum HSI parameter values and resegment the image using the new information. Segmentation quality was assessed by visual inspection, and flower pixels were selected until the segmentation was deemed adequate by human inspection. All supervised segmentations were conducted by the same person to avoid bias in judgment of adequate segmentations. Final values for percent flower cover within the ROI and the minimum and maximum HSI parameters were recorded for each image. This image processing protocol was conducted for 336 and 240 images in 2012 and 2013, respectively, which provided 576 estimates of HSI parameter values that segmented lesquerella flower pixels under multiple irrigation and N fertilization treatments on multiple dates during two growing seasons.

To process the images collected over the final harvest areas, a Monte Carlo sampling technique was used to segment lesquerella flowers while considering uncertainty in the minimum and maximum HSI parameters. Based on the 576 estimates of minimum and maximum HSI from supervised image segmentations, the mean and standard deviation of each parameter were calculated and used to define its normal probability distribution. Using a pseudorandom number generator to iteratively and independently sample values from these normal distributions, HSI parameter values were specified for iterative testing of HSI parameter uncertainty on lesquerella flower segmentation. A total of 500 Monte Carlo parameter samples were evaluated for each image collected over the final harvest areas. No ROIs were specified for these images, so processing was conducted for the full image scene. Results were averaged to provide one estimate of flower cover percentage for each image. This image processing protocol was conducted for 3265 images in 2012 and 2591 images in 2013 to estimate the time course of lesquerella flowering patterns under multiple irrigation and N fertilization treatments.

To verify the accuracy of the Monte Carlo sampling technique, it was also used to evaluate the images collected over the biomass sampling areas. Within the image ROIs, flower cover estimates from the Monte Carlo approach were compared with estimates from the supervised image segmentations. This evidenced the accuracy of the Monte Carlo flower cover estimates with respect to flower cover estimates verified by human inspection.

2.4. Data analysis

Temporal trends in flowering patterns were compared with management and climate factors. Liu et al. (2014) provided the schedules for management of irrigation and N fertilizer during the field studies. Climate data was obtained from an Arizona Meteorological Network station (AZMET; http://ag.arizona.edu/azmet/) less than 1 km from the field site.

To consider the collective temporal pattern of flower count and flower cover percentage within treatment plots, measured values were integrated on a daily basis using linear interpolation to calculate values between measurement dates. This provided a simple metric (i.e., the integral or area under the curve) to summarize the flowering condition in each treatment plot over the flowering period. This "integral metric" was tested in the following statistical analyses.

Hierarchical linear mixed modeling was used to assess differences among flower count and flower cover percentages on each measurement date and among the integral metrics for flower count and flower cover. Water level, N fertilizer rate, and their interaction were modeled as fixed effects. Block and its interaction with water level were modeled as random effects. Hierarchical tests required fitting random effects with (1) water level fixed effects alone, (2) N fertilizer level fixed effects alone, (3) both water and N fertilizer level fixed effects, and (4) water and N fertilizer fixed effects and their interaction. Likelihood ratio tests were used to compare these hierarchical models, which showed whether the measurement was different among water level, N fertilizer rate, or their interaction. Linear mixed models were computed using the "lme4" package within the R Project for Statistical Computing software (http://www.r-project.org).

Simple linear regression models were developed to estimate lesquerella seed yield from flower count, flower cover percentage, and the integral metric. Both the mixed models and the linear models were developed independently for data collected on each measurement date and for the integral metric that summarized the overall temporal flowering condition. The analyses for flower cover percentage used the processing results for images collected over the final harvest areas.
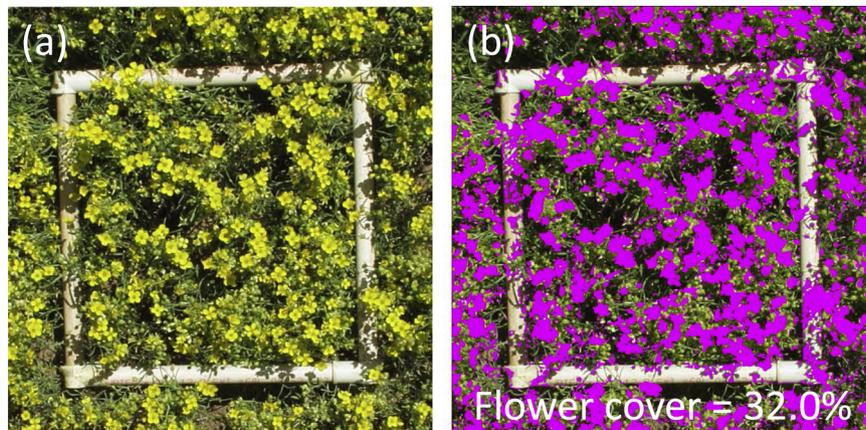
Fig. 1. Example image processing result: (a) original image and (b) image with segmented lesquerella flowers shown in a magenta color. The area of the PVC square was 30 cm × 30 cm. (For interpretation of the references to color in this figure legend, the reader is referred to the web version of this article.)

3. Results and discussion

3.1. Image segmentation

An example of the image processing result is provided in Fig. 1, including a cropped RGB image of a biomass sample area (Fig. 1a) and the resulting image segmentation of lesquerella flowers (Fig. 1b). Pixels identified as flowers after HSI transformation, image segmentation, and 5 × 5 median filtering are marked with a magenta color, and non-flower pixels are shown in their original RGB format. Flower cover for this example image was 32.0%.

The means and standard deviations of the 576 values for minimum and maximum HSI from supervised image segmentations are given in Table 1. Shown for comparison are the HSI results from supervised image segmentations of 105 images in a previous study (Thorp and Dierig, 2011). The means of maximum and minimum hue in the current study were 0.14 and 0.18, respectively. The standard deviations for hue parameters were smaller than that for other parameters, indicating relatively stable yellow hue parameters for lesquerella flower segmentation among images. Two-sample t-tests showed that supervised image segmentations provided different minimum and maximum hue values in the current study as compared to that from the Thorp and Dierig (2011) study ($p < 0.01$). Because the two studies were conducted using different cameras, the differences in hue parameters could be due to differences in the cameras' detectors or color filters. The means of minimum and maximum saturation in the current study were 0.41 and 1.00, respectively. Maximum saturation was always 1.00, indicating fully saturated yellow color was necessary for adequate flower segmentation in all images. A two-sample t-test showed that the mean minimum saturation values in the current study were significantly different from that reported in the

Thorp and Dierig (2011) study ($p < 0.01$). This led to a narrower range of saturation values used for lesquerella flower segmentation in the current study. The means of minimum and maximum intensity in the current study were 0.38 and 0.81, respectively. Mean minimum intensity among the current and previous studies were not different, but the mean maximum intensity was different between the current study and the Thorp and Dierig (2011) study ($p < 0.01$). Differences in minimum and maximum HSI parameters among the two studies could be due to (1) different cameras or (2) different technicians used for supervised image segmentation.

Coefficients of determination (r^2) between each HSI parameter and the resulting flower cover percentage were less than 0.075 (Table 1), indicating low correlation between these variables. Thus, the HSI parameter values did not change with the flower cover condition over the growing season. In the previous study (Thorp and Dierig, 2011), minimum intensity showed a slight correlation with flower cover percentage ($r^2 = 0.277$), which was due to increased flower shading as the canopy developed. The present study did not demonstrate a strong trend for minimum intensity. Because the HSI parameter values from supervised image segmentation were normally distributed (not shown) and not correlated with flowering condition, the Monte Carlo sampling approach used to process images of the final harvest areas is justified. Further justification is provided in the comparison of flower cover percentages from supervised image segmentation and automated segmentation with Monte Carlo sampling for images over the biomass sampling areas (Fig. 2). As compared to segmentations verified by human inspection, the Monte Carlo approach was able to estimate flower cover with RMSEs less than 3.5% and r^2 greater than 0.90 in both growing seasons. Thus, the Monte Carlo technique was able to accurately estimate lesquerella flower cover while also addressing uncertainty in the HSI parameters.

Measured flower count versus flower cover by supervised image segmentation for both growing seasons is shown in Fig. 3. Simple linear regression between the two variables resulted in r^2 of 0.74 and 0.60 for the 2011–2012 and 2012–2013 growing seasons, respectively. These values were lower than that reported by both Adamsen et al. (2000) and Thorp and Dierig (2011). However, the Adamsen et al. (2000) study used less than 30 data points with flower cover up to only 10%, and the Thorp and Dierig (2011) study used 57 data points with flower cover up to 32%. In the current study, results were based on 318 data points in 2011–2012 and 240 data points in 2012–2013. Also, maximum measured flower cover percentages were 48% and 42% in 2011–2012 and 2012–2013, respectively. Thus, the current results were based on a much larger assessment of flower cover variability in the field, and the

Table 1
Descriptive statistics of HSI parameters from supervised image segmentations of lesquerella flowers for the current study and a previous study by Thorp and Dierig (2011). The coefficient of determination (r^2) is computed for each HSI parameter and the resulting percentage of segmented flower pixels.

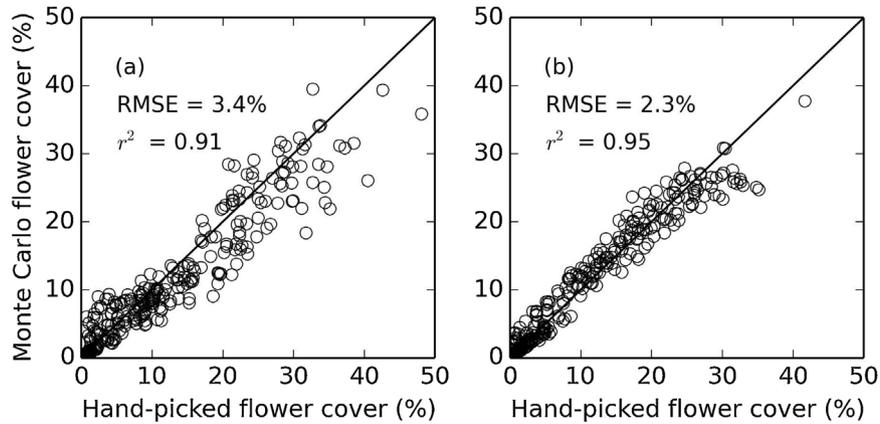|	Current study			Previous study		
	Mean	StDev	r^2	Mean	StDev	r^2
Min Hue	0.1431	0.0063	0.031	0.1216	0.0111	0.002
Max Hue	0.1795	0.0058	0.036	0.1768	0.0084	0.013
Min Sat	0.4075	0.0834	0.067	0.2902	0.0916	0.022
Max Sat	1.0000	0.0000	0.002	1.0000	0.0000	0.086
Min Int	0.3795	0.0520	0.071	0.3763	0.0584	0.277
Max Int	0.8148	0.0371	0.053	0.7513	0.0947	0.003

Fig. 2. Mean flower cover from the Monte Carlo image segmentation procedure versus flower cover from supervised image segmentations for the (a) 2011–2012 and the (b) 2012–2013 growing seasons.
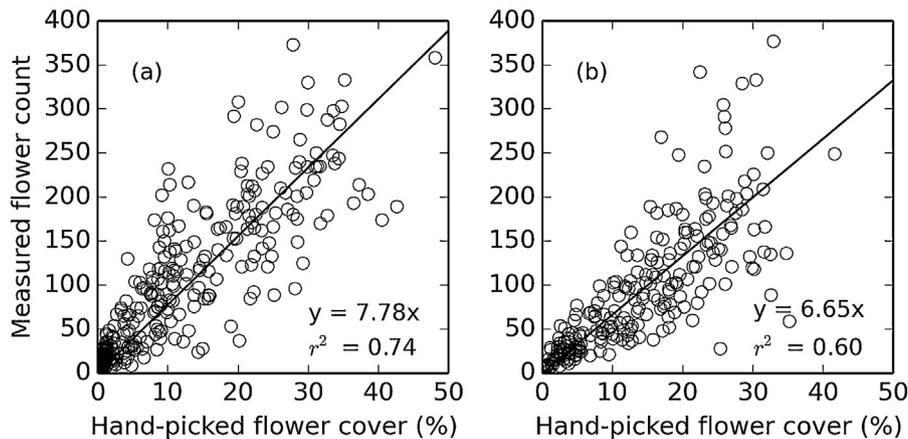

Fig. 3. Regression analysis of measured flower count versus flower cover from supervised image segmentations for the data collected during the (a) 2011–2012 and (b) 2012–2013 growing seasons.

accuracy in estimating flower counts from digital images is likely better demonstrated in the present study than in previous studies.

A substantial portion of the error in the regression models (Fig. 3) was likely due to field sampling issues. Sampling protocol dictated that plants were harvested if their main stem was within the boundary of the 30 cm × 30 cm PVC frame (Fig. 1). Because the whole plant was harvested, branches outside the PVC frame were often included in the sample. Likewise, plants with main stems outside the PVC frame often had branches inside the PVC frame, and these were not included in the sample. By comparison, the image processing procedure analyzed flowers within the PVC boundary, regardless of the plant's main stem location. This discrepancy led to error in the relationship between flower cover percentage and flower counts. The measurement of flower count was problematic due to difficulties in normalizing the data to a known area. On the other hand, flower cover measurements from digital images were easily normalized to a known area by analyzing flowers within ROIs drawn around the inner boundary of the PVC frame.

3.2. Flowering patterns

Because digital images could be rapidly collected and processed, temporal flowering patterns could be monitored in greater detail with the digital imaging approach (Figs. 4 and 5) as compared to manual flower counts (Figs. 6 and 7). This benefit was demonstrated with the flower cover data for the WW treatment during the 2012–2013 season (Fig. 4a). Flower cover increased

for all fertilization levels from 127 days after planting (DAP) to 151 DAP, after which flower cover trended downward over four days to 155 DAP for the lowest four N treatments (N1, N2, N3, and N4) and upward for the two highest N treatments (N5 and N6). Four days later (158 DAP), flower cover trended downward for all N rates except N1. According to the schedules provided by Liu et al. (2014), the WW treatment was irrigated and fertilized on 16 March 2012 (134 DAP), then irrigated on 30 March 2012 (148 DAP), then irrigated and fertilized on 13 April 2012 (162 DAP). Because irrigation occurred at 148 DAP, the initial decline in flower cover percentage from 151 to 155 DAP is likely due to N limitation, which affected only the lowest four N treatments. After 155 DAP, further N shortages reduced flower cover in all N treatments except N1. After the crop was irrigated and fertilized at 162 DAP, flower cover again trended upward for all N fertilization rates. Later in 2012, a similar response occurred with peaks in flower cover on 165 DAP followed by a decline on 168 DAP followed by another peak on 176 DAP. After both the WW and WL treatments were irrigated and fertilized on 13 April 2012 (162 DAP), only the well-water treatment was irrigated again on 23 April 2012 (172 DAP) and only negligible precipitation occurred (1.5 mm on 175 DAP). Thus, the flower cover decline from 165 DAP to 168 DAP is more severe for the WL treatment (Fig. 4b). Also, the substantial rise in flower cover in both the WW and WL treatments from 168 to 176 DAP (Fig. 4) might be explained by daily average temperatures over the period, which were from 3 to 8 °C above average. Trends in flowering during 2012 could be explained by management or climate effects, and the
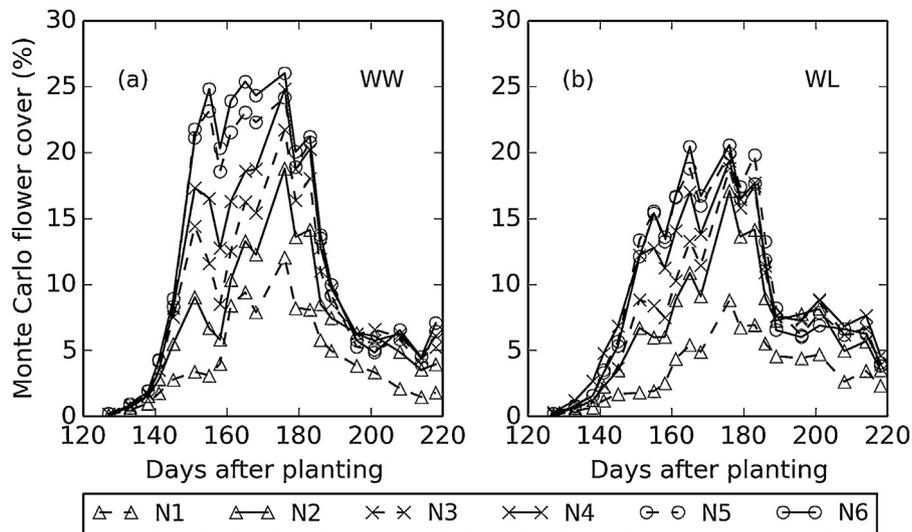
Fig. 4. Mean flower cover percentage under (a) well-watered (WW) and (b) water-limited (WL) conditions for six nitrogen fertilization rates during the 2011–2012 lesquerella experiment.
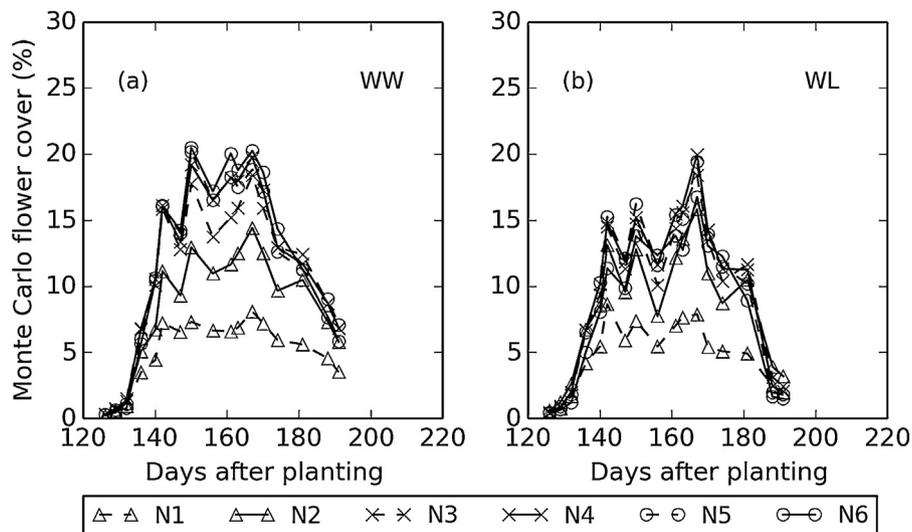

Fig. 5. Mean flower cover percentage under (a) well-watered (WW) and (b) water-limited (WL) conditions for six nitrogen fertilization rates during the 2012–2013 lesquerella experiment.

digital imaging approach provided information with enough detail to link flowering dynamics with a potential cause. On the other hand, manual flower counts were not collected frequently enough to demonstrate clear responses with management or climate trends (Fig. 6).

Compared to 2012, flower development in 2013 occurred earlier. Daily heats units in 2013 from planting to peak flowering (150 DAP) accumulated to 540 degree days (base temperature was 12.8 °C, maximum temperature upper limit was 30 °C), while in 2012 the accumulation from planting to 150 DAP was only 438 degree days. Maximum flower cover percentage with WW conditions at the highest N rate was 20% in 2013 (Fig. 5a) but reached 26% in 2012 (Fig. 4a). Similarly, maximum flower counts were higher for most treatments in 2012 (Fig. 6) as compared to 2013 (Fig. 7), especially for the WL treatment. Higher plant stand density likely contributed to higher flower count and flower cover in 2012.

The 2013 flower cover data also demonstrated responsiveness with management and climate factors (Fig. 5). For example, 2013 flower cover exhibited peaks on 150 DAP for all treatments, but six days later (156 DAP) flower cover declined. The only management

occurring during this time was to irrigate the WW treatment on 153 DAP, and no precipitation occurred. Since the WL treatment was not irrigated during this period, the decline in flower cover is more definitive as compared to the WW treatment. A possible explanation for this pattern in flowering was high reference evapotranspiration from 151 to 155 DAP, which was 38 mm. This was the fifth highest amount over these days for 27 years of weather history at Maricopa. Later in the growing season, flower cover for the WL treatment exhibited a strong peak on 167 DAP (Fig. 5b). This occurred three days after an irrigation event on 164 DAP. Similar to 2012, the frequency of the 2013 flower cover data helped identify potential causes of temporal variations in flowering patterns. Such inferences were not possible with the 2013 flower count data (Fig. 7).

Hierarchical linear mixed modeling demonstrated differences in lesquerella flower count and flower cover that were related to irrigation and N fertilizer management. In 2012, different irrigation schedules among WW and WL treatments were initiated on 91 DAP, but irrigation level did not result in flower cover and flower count differences until 145 DAP and 147 DAP, respectively (Table 2). After
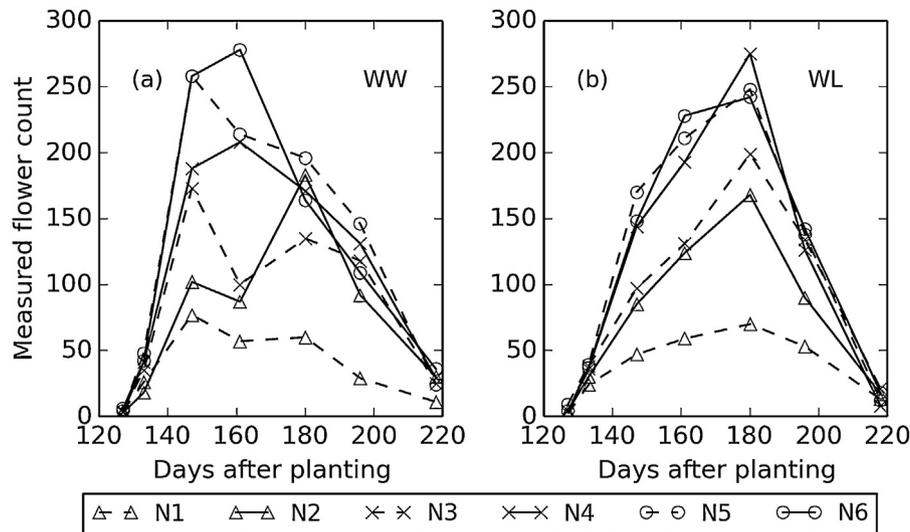
Fig. 6. Mean measured flower count under (a) well-watered (WW) and (b) water-limited (WL) conditions for six nitrogen fertilization rates during the 2011–2012 lesquerella experiment.
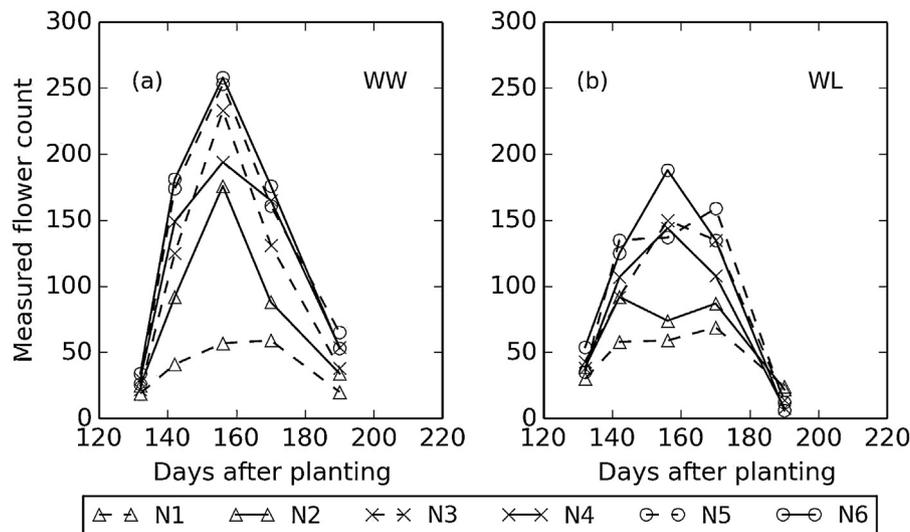

Fig. 7. Mean measured flower count under (a) well-watered (WW) and (b) water-limited (WL) conditions for six nitrogen fertilization rates during the 2012–2013 lesquerella experiment.

145 DAP, flower cover differences among the irrigation treatments were measured on all sampling dates until 186 DAP. The lack of flower cover differences among irrigation treatments on 186 DAP is likely due to the 101 mm irrigation event in both the WW and WL treatment on 183 DAP (Liu et al., 2014). Lesquerella flowering can thus respond quickly to irrigation application, even when the crop was previously water-limited. After 186 DAP, flower cover was often higher in the WL treatment compared to the WW treatment (Fig. 4), perhaps due to higher late-season N availability in the WL treatment. Beginning at 141 DAP in 2012, flower cover was different among N treatments for all subsequent sampling dates. Likewise, flower counts were different among N treatments on four sampling dates from 147 to 196 DAP (Table 2).

Similar results were obtained for the 2013 growing season (Table 3). Flower cover differences among irrigation treatments were present but depended on irrigation timing. For example, the lack of flower cover differences among irrigation treatments on 167 DAP is likely due to the 123 mm irrigation application to both treatments on 164 DAP (Liu et al., 2014). Beginning at 129 DAP in 2013, flower cover was different among N treatments for all

subsequent sampling dates, and flower count was different among N treatments on sampling dates from 142 to 170 DAP in 2013.

3.3. Yield estimation

Flower counts in 2012 (147 DAP) and 2013 (142 and 170 DAP) estimated lesquerella seed yield with r^2 of 0.56 and 0.36, respectively. These were the maximum r^2 values between seed yield and flower counts on a single day (Tables 2 and 3). Maximum r^2 between lesquerella seed yield and flower cover percentages on a single day were 0.81 in 2012 (151, 155, and 168 DAP) and 0.84 in 2013 (163 DAP). During peak bloom from 140 to 180 DAP in both seasons, flower cover percentage from digital images on individual measurement dates consistently estimated lesquerella seed yield better than manual flower counts. As discussed above, issues with the biomass sampling protocol led to error between flower count and flower cover percentage (Fig. 3). Poor seed yield estimates from flower counts can be similarly explained. Because whole plants were harvested if the main stem was within the 30 cm × 30 cm PVC frame, branches outside the PVC frame were often included

Table 2

Statistical analysis results for the 2011–2012 lesquerella growing season, including (1) χ^2 statistics and probability (p) values from hierarchical linear mixed modeling for flower count (top section) and flower cover (bottom section) on selected days after planting (DAP) and for the integral (INT) of interpolated flower count and flower cover over the entire flowering period and (2) coefficients of determination (r^2) for linear models that estimate lesquerella seed yield from flower counts and flower cover percentages.

DAP	Water level			Nitrogen rate			Interaction			r^2
	χ^2	p		χ^2	p		χ^2	p		
127	1.2	0.2814		14.0	0.0155	*	13.3	0.0211	*	0.08
133	0.1	0.8056		8.3	0.1410		1.9	0.8589		0.11
147	12.1	0.0005	***	37.6	0.0000	***	6.4	0.2678		0.56
161	0.0	0.9632		59.6	0.0000	***	5.5	0.3573		0.55
180	9.0	0.0027	**	41.4	0.0000	***	9.9	0.0772		0.15
196	1.1	0.3000		35.4	0.0000	***	3.0	0.6948		0.29
218	6.8	0.0092	**	8.1	0.1512		9.4	0.0935		0.11
INT	0.4	0.5192		79.2	0.0000	***	1.0	0.9659		0.56
127	1.0	0.3093		15.0	0.0105	*	2.7	0.7440		0.15
133	0.0	0.9466		7.1	0.2138		3.5	0.6207		0.10
138	0.2	0.6325		8.1	0.1489		3.9	0.5594		0.09
141	1.0	0.3230		13.9	0.0163	*	3.1	0.6797		0.20
145	9.5	0.0020	**	28.4	0.0000	***	3.1	0.6788		0.40
151	21.0	0.0000	***	83.3	0.0000	***	19.0	0.0018	**	0.81
155	15.4	0.0001	***	89.3	0.0000	***	19.2	0.0018	**	0.81
158	10.0	0.0015	**	77.3	0.0000	***	13.6	0.0185	*	0.75
161	12.1	0.0005	***	66.6	0.0000	***	5.9	0.3183		0.72
165	11.8	0.0006	***	74.3	0.0000	***	2.2	0.8252		0.75
168	20.0	0.0000	***	92.3	0.0000	***	9.2	0.1023		0.81
176	19.5	0.0000	***	102.1	0.0000	***	9.7	0.0830		0.76
179	11.9	0.0006	***	105.8	0.0000	***	9.8	0.0822		0.80
183	6.1	0.0132	*	87.8	0.0000	***	5.2	0.3917		0.78
186	1.6	0.2041		65.9	0.0000	***	3.3	0.6544		0.74
189	6.7	0.0094	**	25.5	0.0001	***	6.2	0.2843		0.47
196	11.1	0.0009	***	45.5	0.0000	***	3.0	0.6971		0.04
201	24.0	0.0000	***	49.6	0.0000	***	5.0	0.4209		0.02
208	1.0	0.3106		93.1	0.0000	***	1.8	0.8799		0.42
214	27.9	0.0000	***	65.5	0.0000	***	6.0	0.3092		0.12
218	9.5	0.0020	**	41.5	0.0000	***	21.9	0.0006	***	0.65
INT	13.5	0.0002	***	94.5	0.0000	***	9.1	0.1053		0.84

Significance codes:
* $p < 0.05$.
** $p < 0.01$.
*** $p < 0.001$.

in the sample (and vice versa), leading to errors in normalizing the data to a known area. Seed yield measurements were less prone to this problem, because yield samples were collected from a $1.5\,m^2$ area, more than 16 times larger than the $30\,cm \times 30\,cm$ ($0.09\,m^2$) area for biomass samples. Digital images for seed yield estimation characterized a much larger portion of the plot area than the areas delineated for biomass or yield samples. For images collected over biomass sampling areas, the $30\,cm \times 30\,cm$ PVC frame contained only 3% of the total image pixels. The image in Fig. 1 was cropped to highlight the biomass sampling area, but the original image covered an area approximately 33 times larger than the biomass sampling area. Thus, an area of approximately $9\,m^2$ was characterized with three digital images at 2 m above the canopy over the final harvest plots. Better lesquerella seed yield estimation with the digital imaging approach was due in part to its ability to characterize flowering patterns over a relatively large portion of the plot area.

The integral of flower count or flower cover measurements (i.e., the area under the curves in Figs. 4–7) often estimated lesquerella seed yield better than measurements on individual days. In 2012 and 2013, the integral of flower count estimated seed yield with r^2 of 0.56 and 0.46, respectively (Fig. 8). The relationship in 2012 was similar to estimating seed yield using flower count data from 147 DAP only (Table 2), but the relationship for 2013 was better than using flower count data for any single measurement date (Table 3). The integral of flower cover percentage estimated seed yield with r^2 of 0.84 in 2012 (Fig. 9), better than that using flower cover data from any single measurement date in that year (Table 2). In 2013, the integral of flower cover estimated seed yield with an r^2 of 0.82 (Fig. 9), better than all single date estimates except
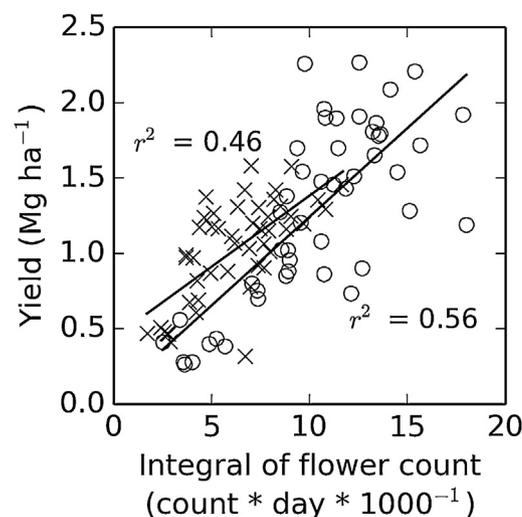

Fig. 8. Lesquerella seed yield versus the integral of interpolated daily flower count estimates during the 2011–2012 (O; $r^2 = 0.56$) and 2012–2013 (X; $r^2 = 0.46$) lesquerella experiments.

163 DAP (Table 3). These results demonstrate a clear advantage for techniques that track the dynamics of lesquerella flowering over time, because lesquerella flowering patterns can change rapidly over several days due to effects of environment and management. Furthermore, approaches that permit frequent monitoring are better able to detect these changes at finer time scales, which lead

Table 3
Statistical analysis results for the 2012–2013 lesquerella growing season, including (1) χ^2 statistics and probability (p) values from hierarchical linear mixed modeling for flower count (top section) and flower cover (bottom section) on selected days after planting (DAP) and for the integral (INT) of interpolated flower count and flower cover over the entire flowering period and (2) coefficients of determination (r^2) for linear models that estimate lesquerella seed yield from flower counts and flower cover percentages.

DAP	Water level			Nitrogen rate			Interaction			r^2
	χ^2	p		χ^2	p		χ^2	p		
132	8.0	0.0047	**	9.0	0.1085		1.9	0.8586		0.00
142	5.1	0.0244	*	32.1	0.0000	***	5.8	0.3235		0.36
156	4.6	0.0312	*	20.5	0.0010	**	3.5	0.6263		0.21
170	2.4	0.1213		38.1	0.0000	***	8.0	0.1546		0.36
190	11.8	0.0006	***	4.2	0.5188		25.8	0.0001	***	0.13
INT	9.7	0.0018	**	59.1	0.0000	***	13.7	0.0175	*	0.46
126	9.1	0.0025	**	10.7	0.0572		12.2	0.0327	*	0.04
129	8.5	0.0036	**	11.9	0.0358	*	10.7	0.0567		0.04
132	12.8	0.0004	***	22.9	0.0004	***	11.4	0.0447	*	0.00
136	0.6	0.4569		30.6	0.0000	***	6.8	0.2379		0.37
140	0.1	0.7310		44.2	0.0000	***	9.9	0.0775		0.66
142	1.4	0.2298		40.9	0.0000	***	12.4	0.0294	*	0.65
147	6.7	0.0097	**	54.6	0.0000	***	10.8	0.0553		0.76
150	7.3	0.0069	**	58.6	0.0000	***	14.4	0.0133	*	0.74
156	22.8	0.0000	***	98.5	0.0000	***	18.5	0.0024	**	0.64
161	9.9	0.0016	**	83.6	0.0000	***	32.3	0.0000	***	0.81
163	5.3	0.0213	*	67.6	0.0000	***	27.2	0.0001	***	0.84
167	0.2	0.6242		83.5	0.0000	***	9.6	0.0887		0.78
170	11.9	0.0006	***	92.6	0.0000	***	14.0	0.0154	*	0.78
174	8.5	0.0035	**	92.2	0.0000	***	4.5	0.4801		0.65
181	6.8	0.0090	**	90.8	0.0000	***	9.0	0.1098		0.68
188	36.0	0.0000	***	24.8	0.0002	***	70.5	0.0000	***	0.14
191	33.6	0.0000	***	21.9	0.0005	***	37.5	0.0000	***	0.13
INT	12.9	0.0003	***	86.2	0.0000	***	24.1	0.0002	***	0.82

Significance codes:
* $p < 0.05$.
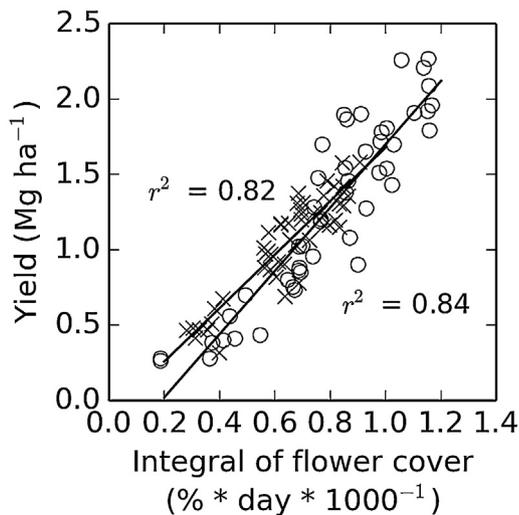** $p < 0.01$.
*** $p < 0.001$.

Fig. 9. Lesquerella seed yield versus the integral of interpolated daily flower cover estimates during the 2011–2012 (O; $r^2 = 0.84$) and 2012–2013 (X; $r^2 = 0.82$) lesquerella experiments.

to better seed yield estimates. For fall-planted lesquerella, results for the digital imaging approach suggest that any single outing to measure flower cover from 150 to 180 DAP provided reasonable estimates of seed yield ($r^2 > 0.60$). However, the best day for measurements likely depends on conditions specific to the growing season and would be difficult to determine in real-time. By integrating twice weekly measurements of flower cover over the growing season, the best seed yield estimates were consistently obtained ($r^2 > 0.80$). Thus, techniques that integrate frequent measurements of lesquerella flowering provide better information to

characterize seed yield as compared to measurements at a single time points.

4. Conclusions

Temporal patterns of lesquerella flowering can be characterized using a commercial digital camera to collect digital images of the crop canopy. By transforming the images from RGB to HSI color space, pixels representing lesquerella flowers can be segmented from background pixels, and the flower cover percentage can be calculated. Compared to sampling biomass for manual flower counts, digital image collection and analysis required less human effort, and 100 times more crop area could be sampled 3 times more often. More frequent observations using digital images revealed temporal flowering dynamics that could be explained by management practices. Because the lesquerella flowering process is very dynamic, observations of the flowering condition must occur twice per week or at even finer time scales to adequately characterize temporal responses of flower development. Water and N limitations were shown to affect both flower count and flower cover. Thus, the imaging approach could be further developed as a tool to assist irrigation and fertilizer management decisions or to select lesquerella varieties that perform better during periods of water or N stress. Such tools are particularly relevant for irrigated desert agriculture, where weekly irrigation management decisions are required. Due in part to the larger sampling area for the digital imaging approach, flower cover consistently estimated lesquerella seed yield better than manual flower counts, particularly during the period of peak flowering. Furthermore, the integral of flower cover measurements over time generally estimated seed yield better than flower cover on a single measurement date. This demonstrated the importance of temporal flowering patterns in the formation of harvestable seed yield. Overall, the temporal

dynamics of lesquerella flowering was affected by water and N limitation and was strongly correlated with seed yield in two growing seasons. As compared to counting flowers manually, segmentation of lesquerella flowers in digital images, collected twice weekly, provided more data for better characterization of lesquerella flowering patterns.

Acknowledgments

References

Adamsen, F.J., Coffelt, T.A., Nelson, J.M., 2003. Flowering and seed yield of lesquerella as affected by nitrogen fertilization and seeding rate. Ind. Crops Prod. 18 (2), 125–131.

Adamsen, F.J., Coffelt, T.A., Nelson, J.M., Barnes, E.M., Rice, R.C., 2000. Method for using images from a color digital camera to estimate flower number. Crop Sci. 40 (3), 704–709.

Dierig, D.A., Adam, N.R., Mackey, B.E., Dahlquist, G.H., Coffelt, T.A., 2006. Temperature and elevation effects on plant growth, development, and seed production of two lesquerella species. Ind. Crops Prod. 24 (1), 17–25.

Dierig, D.A., Thompson, A.E., Nakayama, F.S., 1993. Lesquerella commercialization efforts in the United States. Ind. Crops Prod. 1 (4), 289–293.

Dierig, D.A., Wang, G., McCloskey, W.B., Thorp, K.R., Isbell, T.A., Ray, D.T., Foster, M.A., 2011. Lesquerella: new crop development and commercialization in the U.S. Ind. Crops Prod. 34 (2), 1381–1385.

Dierig, D.A., Wang, G.S., Crafts Brandner, S.J., 2012. Dynamics of reproductive growth of lesquerella (Physaria fendleri) over different planting dates. Ind. Crops Prod. 35 (1), 146–153.

Geller, D.P., Goodrum, J.W., 2004. Effects of specific fatty acid methyl esters on diesel fuel lubricity. Fuel 83 (17–18), 2351–2356.

Gonzalez, R.C., Woods, R.E., 1992. Digital Image Processing. Addison-Wesley Publishing Company, Inc.

Hunsaker, D.J., Nakayama, F.S., Dierig, D.A., Alexander, W.L., 1998. Lesquerella seed production: water requirement and management. Ind. Crops Prod. 8 (2), 167–182.

Liu, J., Bronson, K.F., Thorp, K.R., Mon, J., Badaruddin, M., McCloskey, W.B., Ray, D.T., Chu, Q., Wang, G., 2014. Lesquerella seed and oil yield response to split-applied N fertilizer. Ind. Crops Prod. 60, 273–279.

Moser, B.R., Cermak, S.C., Isbell, T.A., 2008. Evaluation of castor and lesquerella oil derivatives as additives in biodiesel and ultralow sulfur diesel fuels. Energy Fuels 22 (2), 1349–1352.

Nelson, J.M., Dierig, D.A., Nakayama, F.S., 1996. Planting date and nitrogen fertilization effects on lesquerella production. Ind. Crops Prod. 5 (3), 217–222.

Nelson, J.M., Watson, J.E., Dierig, D.A., 1999. Nitrogen fertilization effects on lesquerella production. Ind. Crops Prod. 9 (3), 163–170.

Ploschuk, E.L., Cerdeiras, G., Windauer, L., Dierig, D.A., Ravetta, D.A., 2003. Development of alternative Lesquerella species in Patagonia (Argentina): potential of Lesquerella angustifolia. Ind. Crops Prod. 18 (1), 1–6.

Puppala, N., Fowler, J.L., Jones, T.L., Gutschick, V., Murray, L., 2005. Evapotranspiration, yield, and water-use efficiency responses of Lesquerella fendleri at different growth stages. Ind. Crops Prod. 21 (1), 33–47.

Roseberg, R.J., 1993. Cultural-practices for lesquerella production. J. Am. Oil Chem. Soc. 70 (12), 1241–1244.

Roseberg, R.J., 1996. Herbicide tolerance and weed control strategies for lesquerella production. Ind. Crops Prod. 5 (2), 133–139.

Smith, C.R., Zobel, H., Wolff, I.A., Miwa, T.K., Wilson, T.L., Lohmar, R.L., 1961. Lesquerolic acid – a new hydroxy acid from lesquerella seed oil. J. Org. Chem. 26 (8), 2903–2905.

Thorp, K.R., Dierig, D.A., 2011. Color image segmentation approach to monitor flowering in lesquerella. Ind. Crops Prod. 34 (1), 1150–1159.